CONFIDENTIAL

SEP 25 1958

Copy 238

RM A58F30

NACA

RESEARCH MEMORANDUM

INVESTIGATION OF WINGLESS MISSILE CONFIGURATIONS WITH FOLDING CONTROLS AND LOW-ASPECT-RATIO STABILIZING SURFACES

By Frank A. Lazzeroni

Ames Aeronautical Laboratory
Moffett Field, Calif.

NATIONAL ADVISORY COMMITTEE FOR AERONAUTICS

WASHINGTON

September 17, 1958

CONFIDENTIAL

NATIONAL ADVISORY COMMITTEE FOR AERONAUTICS

RESEARCH MEMORANDUM

INVESTIGATION OF WINGLESS MISSILE CONFIGURATIONS WITH FOLDING CONTROLS AND LOW-ASPECT-RATIO STABILIZING SURFACES*

By Frank A. Lazzeroni

SUMMARY

A wind-tunnel investigation has been made of wingless missile configurations having cylindrical bodies and conical or hemispherical noses, extensible control surfaces aft of the nose, and tails consisting of eight low-aspect-ratio triangular or rectangular fins. Normal-force, axial-force, and pitching-moment coefficients were obtained for various control deflections up to a maximum of 30° for Mach numbers of 1.2 and 1.9.

The results of the investigation indicate that the tail-on configurations had adequate static stability in pitch at the Mach numbers tested for a center of gravity at 56.5 percent of the body length. For particular center-of-gravity locations chosen, the control surface on the conical-nosed body was the most effective of all the configurations tested particularly at angles of attack above zero. Changing the tail configuration on the hemispherical-nosed body by substituting rectangular fins for triangular fins had a negligible effect on control effectiveness.

INTRODUCTION

The use of large-span wings on air-to-air guided missiles may result in performance penalties on missile-carrying fighter aircraft because of increased airplane drag due to externally mounted missiles or large airplane volume needed to store the weapons internally. A reduction in size of missile wings would reduce stowage drag. If the wings could be eliminated entirely and replaced by folding controls and stabilizing surfaces, a twofold gain could result; first, stowage drag would be reduced and, second, the missiles could be launched from a tube which should aid in reducing launching errors. Results of some previous experimental investigations of wingless missile configurations are presented in references 1

*Title, Unclassified

through 4. These results show that large-span wings may not be necessary to provide adequate lift for maneuvering, especially at high Mach numbers.

The investigation reported herein was conducted to determine the feasibility of a body flap on a configuration similar to that presented in reference 2 which utilized a control that was a deflectable segment of a conical nose. Moving the control surface onto the body aft of the nose would provide additional room in the nose for warhead and seeker equipment. In addition, a similar body flap was investigated on a wingless hemispherical-nosed body. Such a nose shape may be required in preference to a conical nose for increased efficiency of operation of some seeker systems.

The control surface on each configuration was a deflectable section of the surface of the cylindrical body. Stabilizing surfaces were provided at the aft end of the body and consisted of eight low-aspect-ratio fins. Force and moment characteristics were obtained for flap deflections up to 30° at Mach numbers of 1.2 and 1.9 and angles of attack up to 20°.

SYMBOLS

C_c	axial-force coefficient, $\frac{\text{axial force}}{qS}$
C_m	pitching-moment coefficient, $\frac{\text{pitching moment}}{qSd}$
C_N	normal-force coefficient, $\frac{\text{normal force}}{qS}$
C_{m_α}	pitching-moment-curve slope, per deg
ΔC_m	incremental pitching-moment coefficient due to control-surface deflection
c.g.	center of gravity
d	body diameter, ft
l	body length, ft
M	free-stream Mach number
q	free-stream dynamic pressure, lb/sq ft
R	Reynolds number based on body diameter
S	maximum cross-sectional area of body, sq ft

α angle of attack of longitudinal center line of body, deg

δ angle of deflection of control surface measured with respect to the surface of the body, deg

APPARATUS, MODELS, AND TEST PROCEDURE

The experimental investigation was conducted in the Ames 6- by 6-foot supersonic wind tunnel. In this wind tunnel the Mach number can be varied continuously and the stagnation pressure can be regulated to maintain a given test Reynolds number. A description of the wind tunnel and its stream characteristics is given in detail in reference 5.

Pertinent model areas and sketches of the configurations tested are shown in the following table I and figure 1, respectively. Model A

Configuration	Control-surface area, ft^2	Body cross-section area, ft^2	Exposed area, one fin, ft^2
Model A	0.1047	0.0707	0.0521
Model B	.1047	.0707	---
Model C	.0707	.0707	.0521
Model D	.0707	.0707	.1042
Model E	.0707	.0707	---

consisted of a cylindrical body in conjunction with a conical nose and eight low-aspect-ratio triangular-shape fins mounted on the aft end of the body. Model B was simply the same configuration with the tail removed. Model C was constructed by substituting a hemispherical nose in place of the conical nose of model A. In addition, the model with the hemispherical nose was tested with eight low-aspect-ratio rectangular fins in place of the triangular fins. This particular configuration was designated model D (fig. 2). Model E was the tail-off configuration of either model C or D. Both the triangular and rectangular fins were constructed of constant thickness (0.125 in.) flat plate with leading edges rounded (L.E. radius = 0.0625 in.). All models were sting mounted and the normal forces, axial forces, and pitching moments were measured by means of an electrical strain-gage balance contained within the body of the model. A Reynolds number of 0.77 million (based on body diameter) was maintained at the test Mach numbers of 1.2 and 1.9.

REDUCTION OF DATA

The test data have been reduced to standard NACA coefficient form. Factors which could affect the accuracy of these data, and the corrections applied, are discussed in the following paragraphs.

The present investigation was conducted prior to the modifications to the 6- by 6-foot supersonic wind tunnel which extended the Mach number range. A survey of the tunnel at supersonic speeds (ref. 5) showed the presence of some stream-angle variations in vertical planes but little in horizontal planes. To minimize the effects of these stream irregularities, the models were pitched in the horizontal plane of the tunnel where the most favorable flow conditions existed. A variation in the static pressure along the tunnel caused the models to experience a buoyant force in the chordwise direction. Corrections for this buoyancy were applied to the axial-force data obtained. As a result of pitching the models in the horizontal plane of the tunnel, no direct measurement of the angle of attack of the models was possible. Determination of the true angle of attack consisted of calibrating the movement of the sting in the horizontal plane and adding to this a correction to account for the deflection of the sting-model combination under load.

The following table lists the estimated uncertainties in the measurements, exclusive of the effects of stream-angle variations:

Quantity	Accuracy
C_c	±0.01
C_m	±0.02
C_N	±0.04
M	±0.01
R	$\pm 0.03 \times 10^6$
α	$\pm 0.1^\circ$

RESULTS AND DISCUSSION

The results of the investigation in the form of normal-force, pitching-moment, and axial-force coefficients are presented in figures 3 through 8. A study of these data shows that for the Mach numbers of this test the pitching-moment effectiveness of the control surfaces on all the configurations is approximately independent of Mach number at angles of attack near zero. The static stability in pitch of the tail-on configurations is adequate at the Mach numbers investigated for the center of gravity at 56.5 percent of the body length. However, the control surfaces are capable of developing only small normal forces (figs. 3, 4, and 5) and the axial force accompanying control-surface deflection is generally high (see fig. 8). The high degree of nonlinearity present in the

pitching-moment curves of the tail-on configurations (figs. 3, 4, and 5) is due to the movement of the center of pressure with angle of attack. These curves are more nonlinear for models C and D than for model A which implies a larger movement of the center of pressure for the hemispherical-nosed configurations. In general, changing from a conical nose to a hemispherical nose decreases the static stability in pitch and increases the axial force. However, at angles of attack above zero, the control effectiveness of the hemispherical-nosed configuration increases with Mach number while the control effectiveness of the conical-nose configuration decreases.

In order that the effectiveness of the controls on the various configurations be comparable, the pitching-moment data were adjusted for different center-of-gravity positions (see figs. 9 and 10). The criterion used to select the new center-of-gravity locations was that through the range of trim-lift coefficients, the static stability of the tail-on configurations, $-C_{m_\alpha}$, be equal to or greater than 0.10 at a Mach number of 1.9. The pitching-moment effectiveness of each control is presented in figures 11 and 12 for the tail-on and corresponding tail-off configurations, respectively. Tail-off data are presented since the presence of stabilizing surfaces in the flow behind the controls may affect the results in varying degrees as shown by comparing figures 11 and 12. In addition to the data of the present report, the results from reference 3 are also presented for comparison purposes.[1] As shown in figure 12, despite its smaller moment arm, the control on the conical-nosed body of the present report is more effective than that on the hemispherical-nosed body. At zero angle of attack the effectiveness is approximately proportional to the surface area of the control (see table I); however, at 10° angle the effectiveness increases for the conical-nosed model but not for the hemispherical-nosed models. By comparison, the effectiveness of the control from reference 2 is somewhat higher than any of the configurations of the present report because it is on the nose cone in a region of higher pressure and at an initial angle.

A comparison of models C and D (figs. 9(b) and 9(c)) shows that the control effectiveness was the same for the two tail configurations investigated in conjunction with the hemispherical-nosed body. However, model D has somewhat higher trim-lift capabilities at $M = 1.9$. In addition, the pitching-moment characteristics of model D are somewhat more nonlinear than those of model C, indicating larger center-of-pressure travel with the rectangular fins than with the triangular fins.

[1]These data are also obtained from adjusted pitching-moment curves corresponding to a new center-of-gravity location for $-C_{m_\alpha} \geq 0.10$ at M=1.9.

CONCLUDING REMARKS

Results of an experimental investigation of wingless missile configurations have been presented. These results indicate that the tail-on configurations had adequate static stability in pitch at the Mach numbers tested for a center of gravity at 56.5 percent of the body length. For particular center-of-gravity locations chosen such that the minimum value of pitching-moment-curve slope at trim was -0.10, the control on the conical-nosed body was more effective than that on the hemispherical-nosed body particularly at angles of attack above zero. Changing the tail configuration on the hemispherical-nosed body by substituting rectangular fins for triangular fins had a negligible effect on control effectiveness.

For a more complete evaluation of the present configurations, further investigations would have to be made concerning, for example, the dynamic behavior of these airframes and their tracking capabilities as part of a missile system. The results of a simulation study of a wingless missile with the extensible control surface on the conical nose are presented in reference 6. It was found that the tracking capabilities compared quite favorably with those of a conventional winged cruciform missile.

Ames Aeronautical Laboratory
National Advisory Committee for Aeronautics
Moffett Field, Calif., June 30, 1958

REFERENCES

1. Reese, David E., Jr.: A Wind-Tunnel Investigation of Several Wingless Missile Configurations at Supersonic Speeds. NACA RM A57J22, 1958.

2. Lazzeroni, Frank A.: Investigation of a Missile Airframe With Control Surfaces Consisting of Projecting Quadrants of the Nose Cone. NACA RM A53L21, 1954.

3. Eggers, A. J., Jr., and Syvertson, Clarence A.: Experimental Investigation of a Body Flare for Obtaining Pitch Stability and a Body Flap for Obtaining Pitch Control in Hypersonic Flight. NACA RM A54J13, 1955.

4. Gloria, Hermilo R.: An Experimental Investigation of the Static Longitudinal Stability and Control Characteristics of a Wingless Missile Configuration at Mach Numbers From 3.0 to 6.3. NACA RM A58C20, 1958.

5. Frick, Charles W., and Olson, Robert N.: Flow Studies in the Asymmetric Adjustable Nozzle of the Ames 6- by 6-Foot Supersonic Wind Tunnel. NACA RM A9E24, 1949.

6. Lessing, Henry C., and Reese, David E., Jr.: A Simulation Study of a Wingless Missile. NACA RM A55L06, 1956.

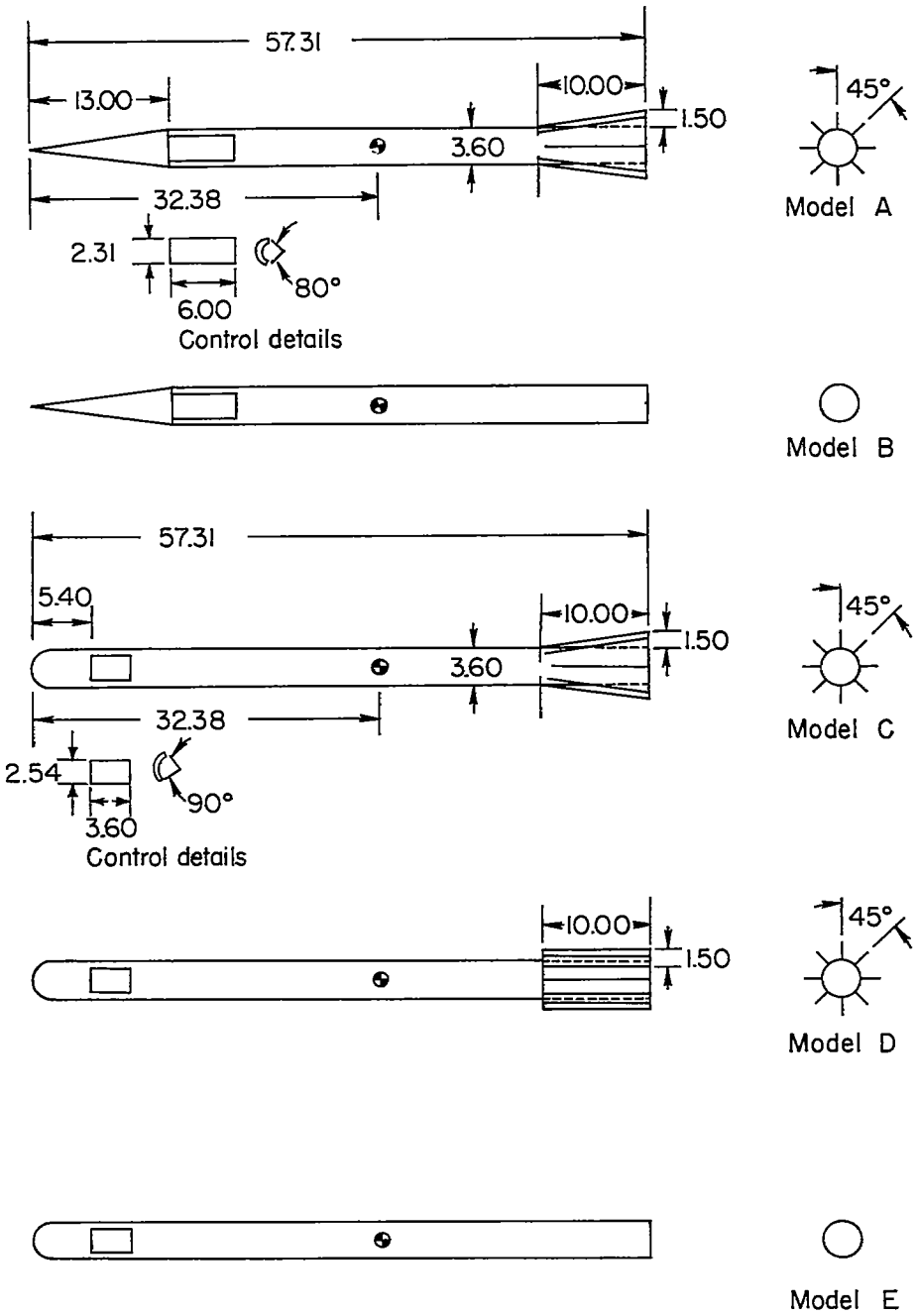

Figure 1.- Sketches of models.

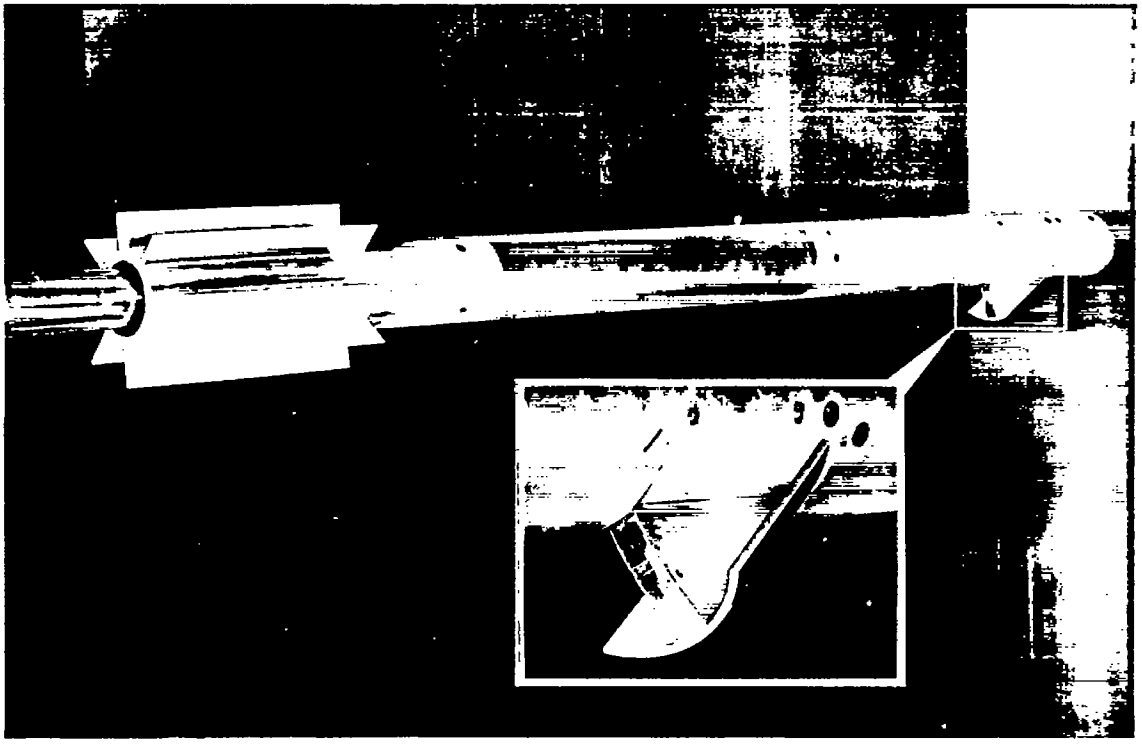

A-19311

Figure 2.- Photograph of model D.

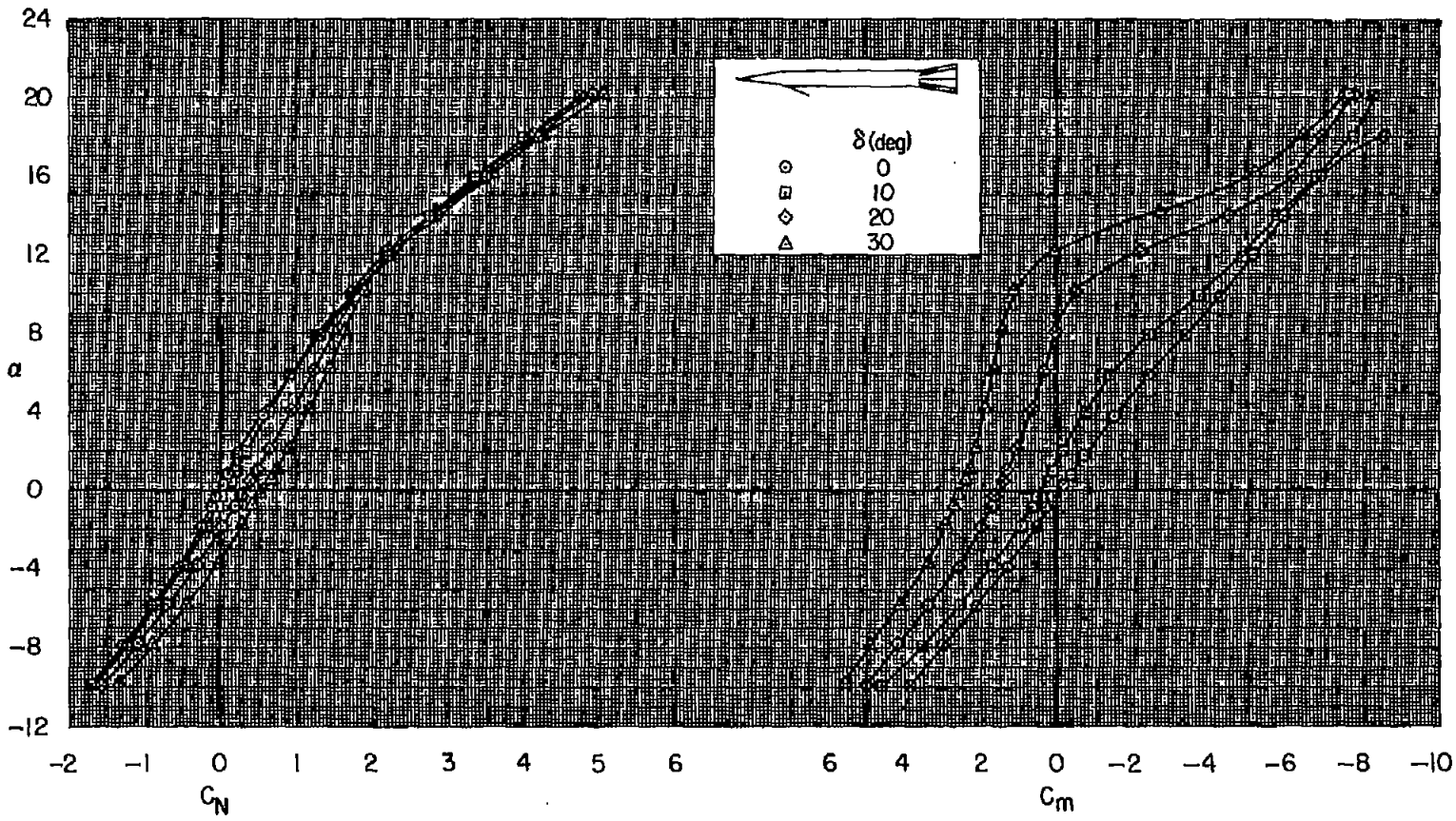

(a) M = 1.2

Figure 3.- Normal-force and pitching-moment characteristics of model A.

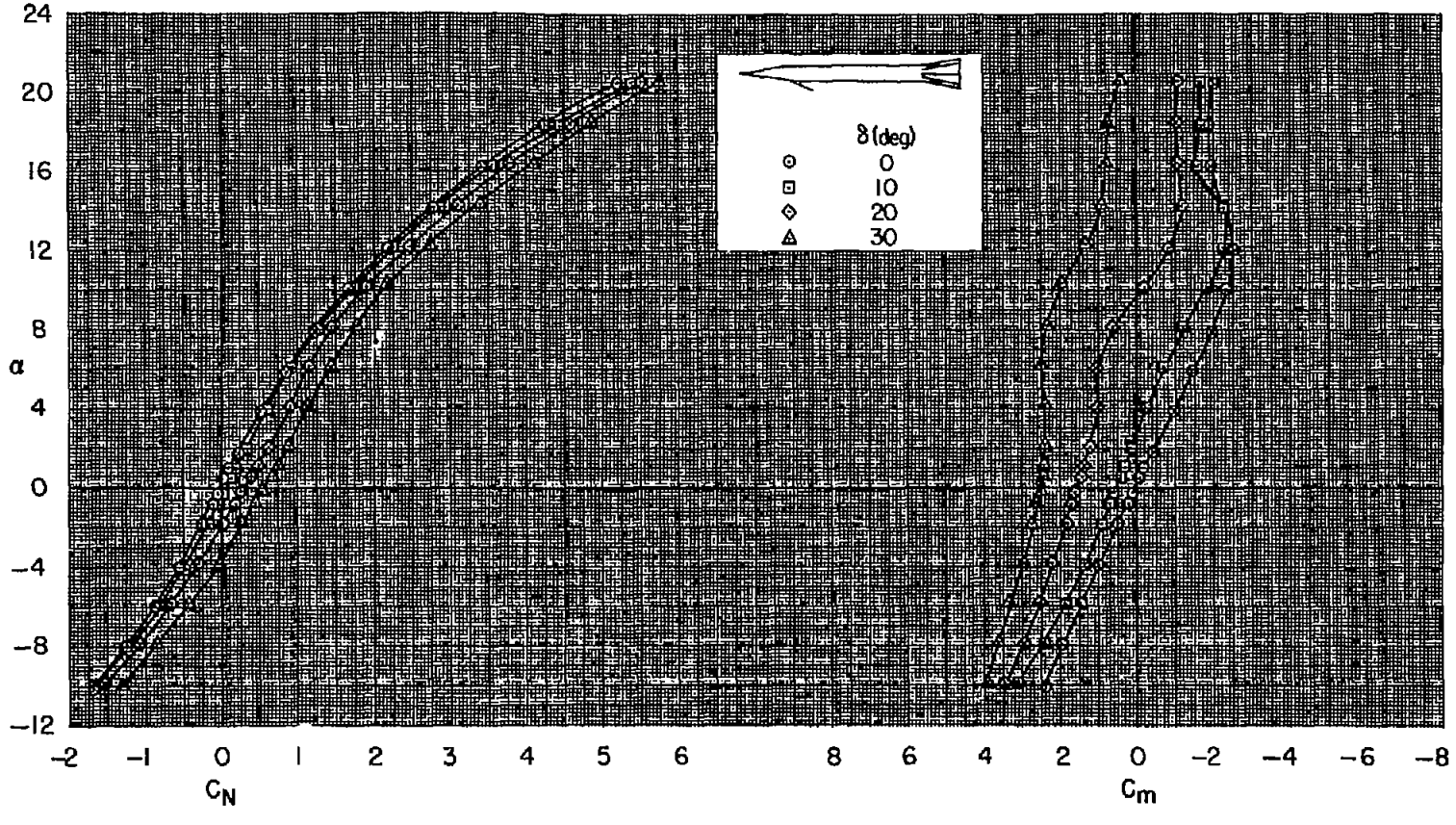

(b) M = 1.9

Figure 3.- Concluded.

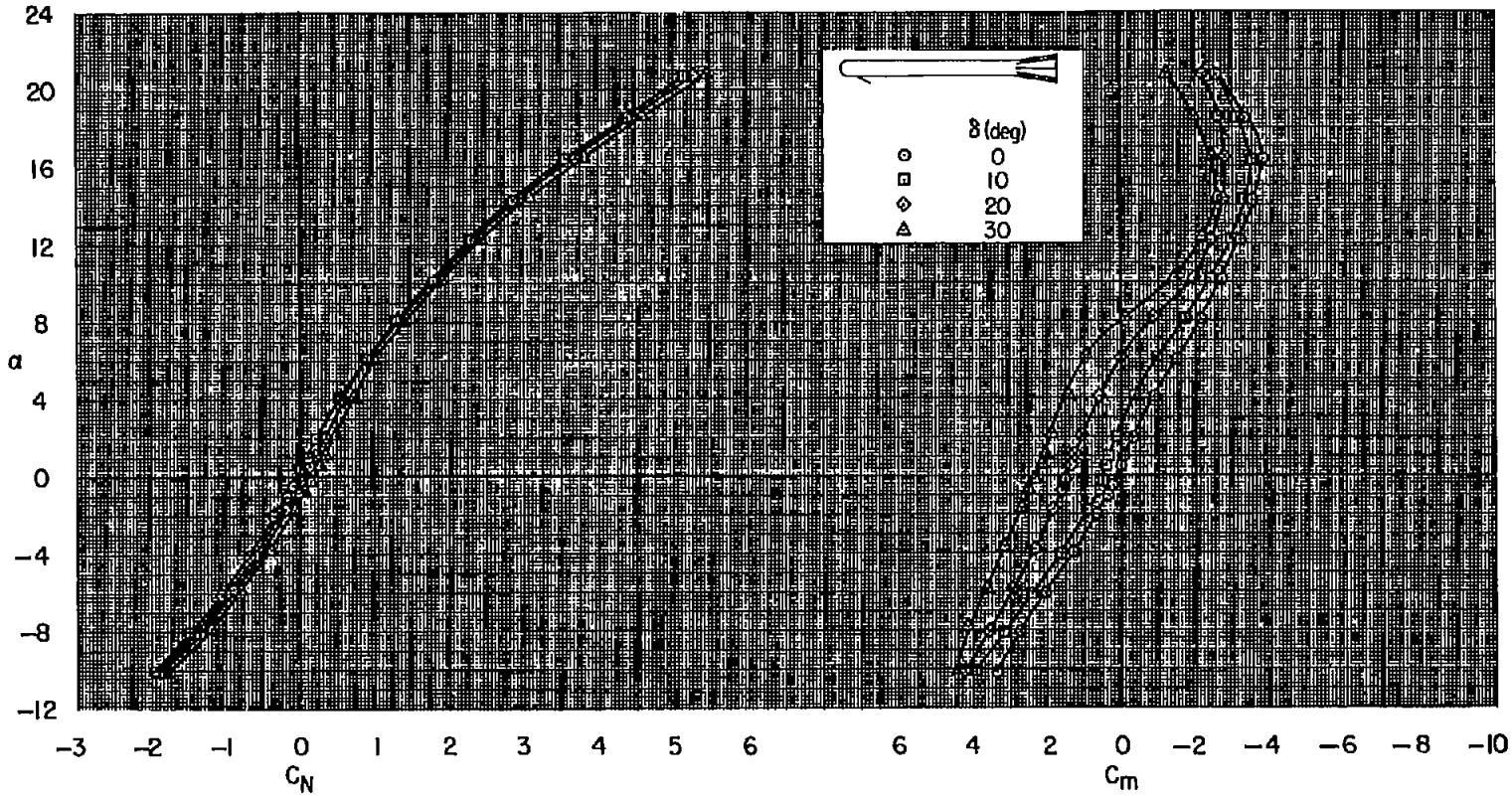

(a) M = 1.2

Figure 4.- Normal-force and pitching-moment characteristics of model C.

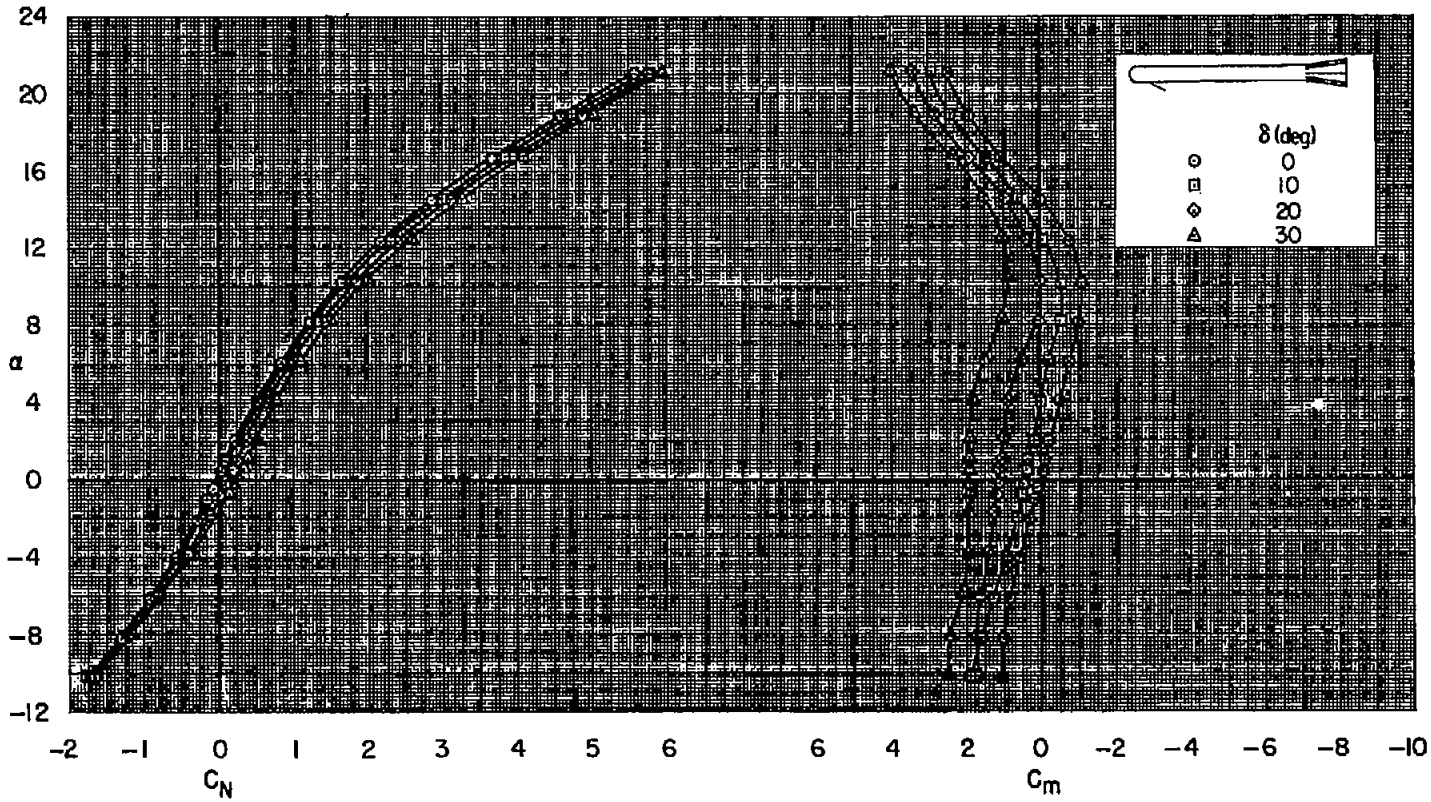

(b) M = 1.9

Figure 4.- Concluded.

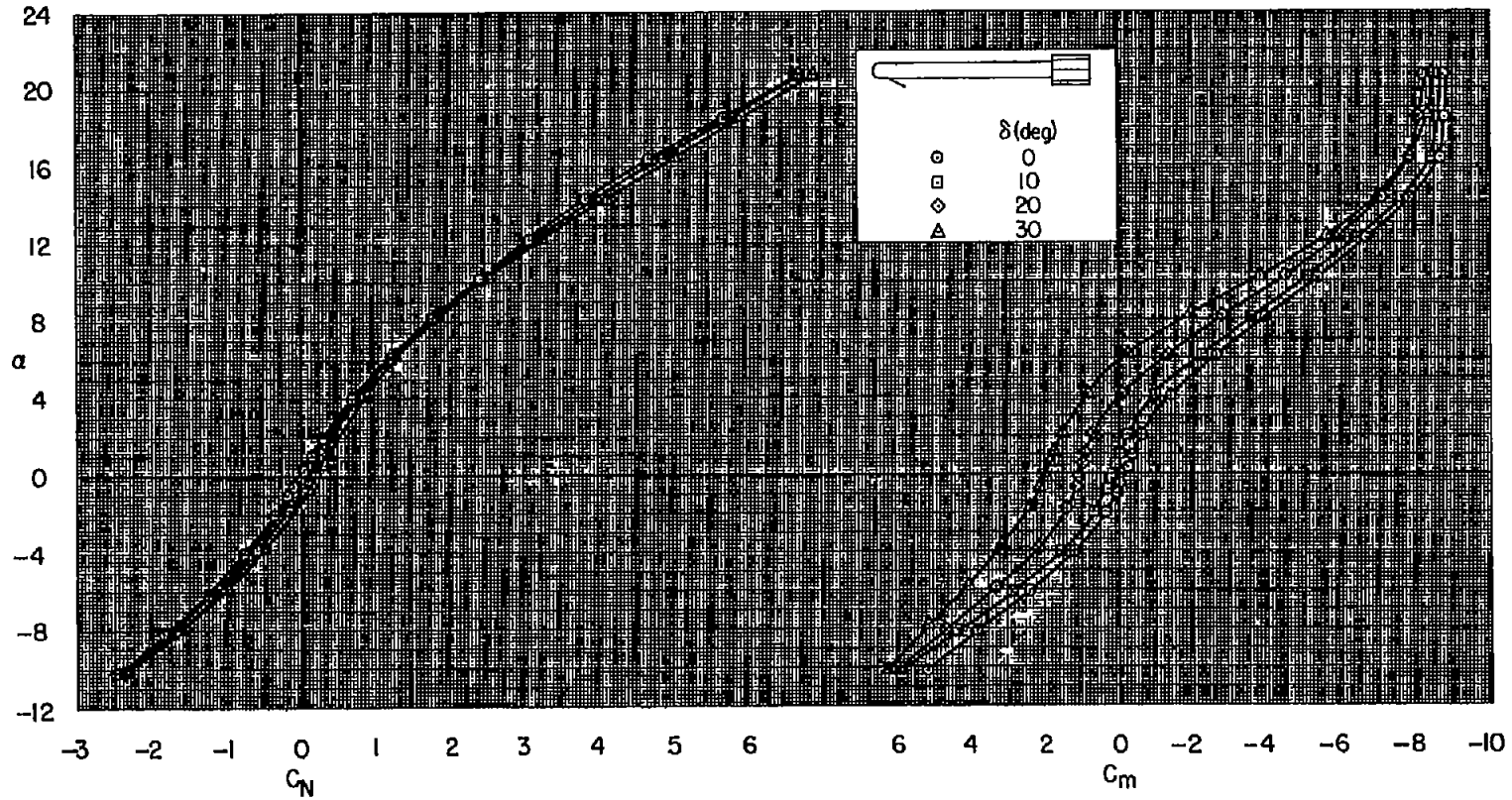

(a) M = 1.2

Figure 5.- Normal-force and pitching-moment characteristics of model D.

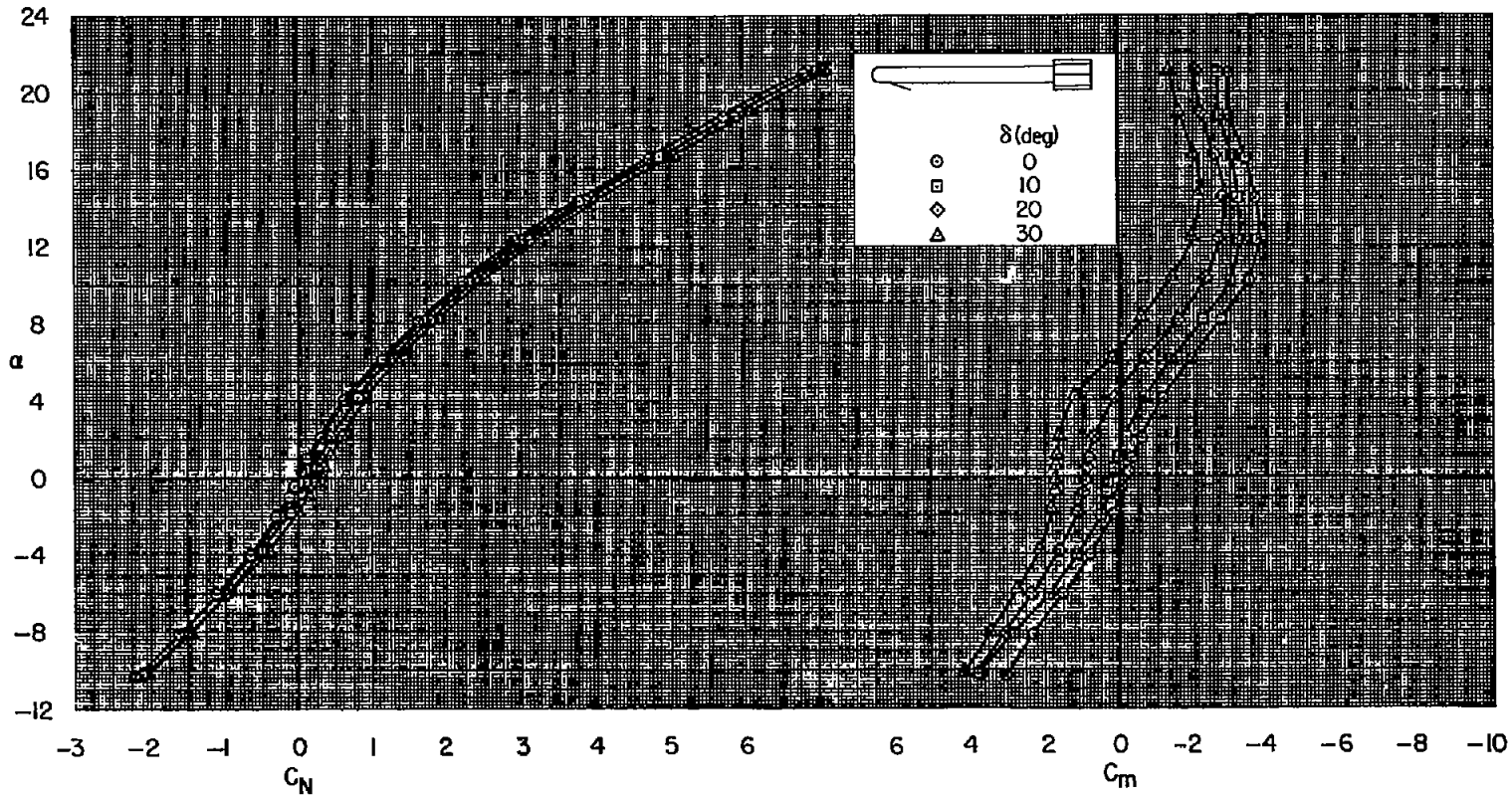

(b) M = 1.9

Figure 5.- Concluded.

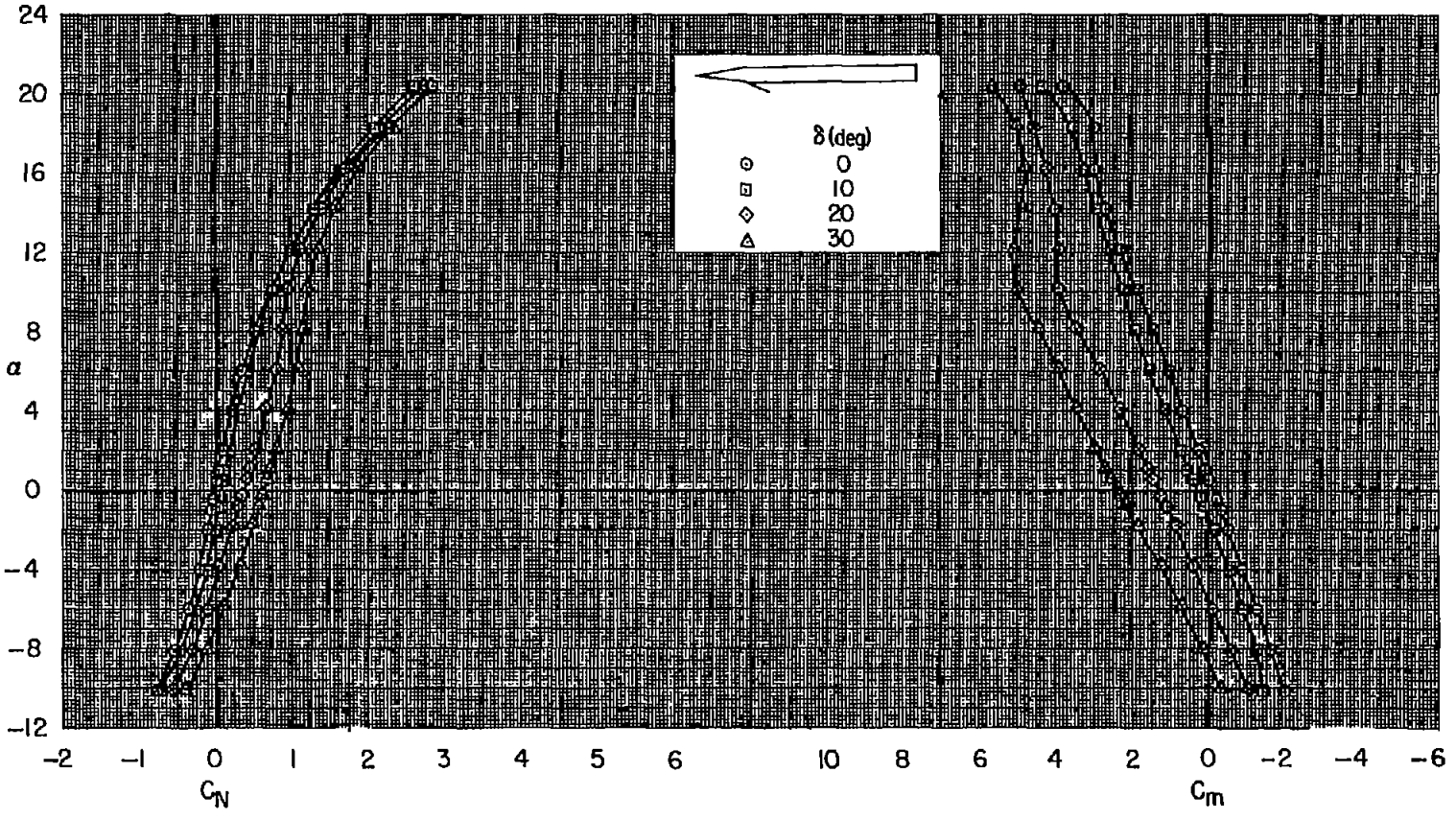

(a) M = 1.2

Figure 6.- Normal-force and pitching-moment characteristics of model B.

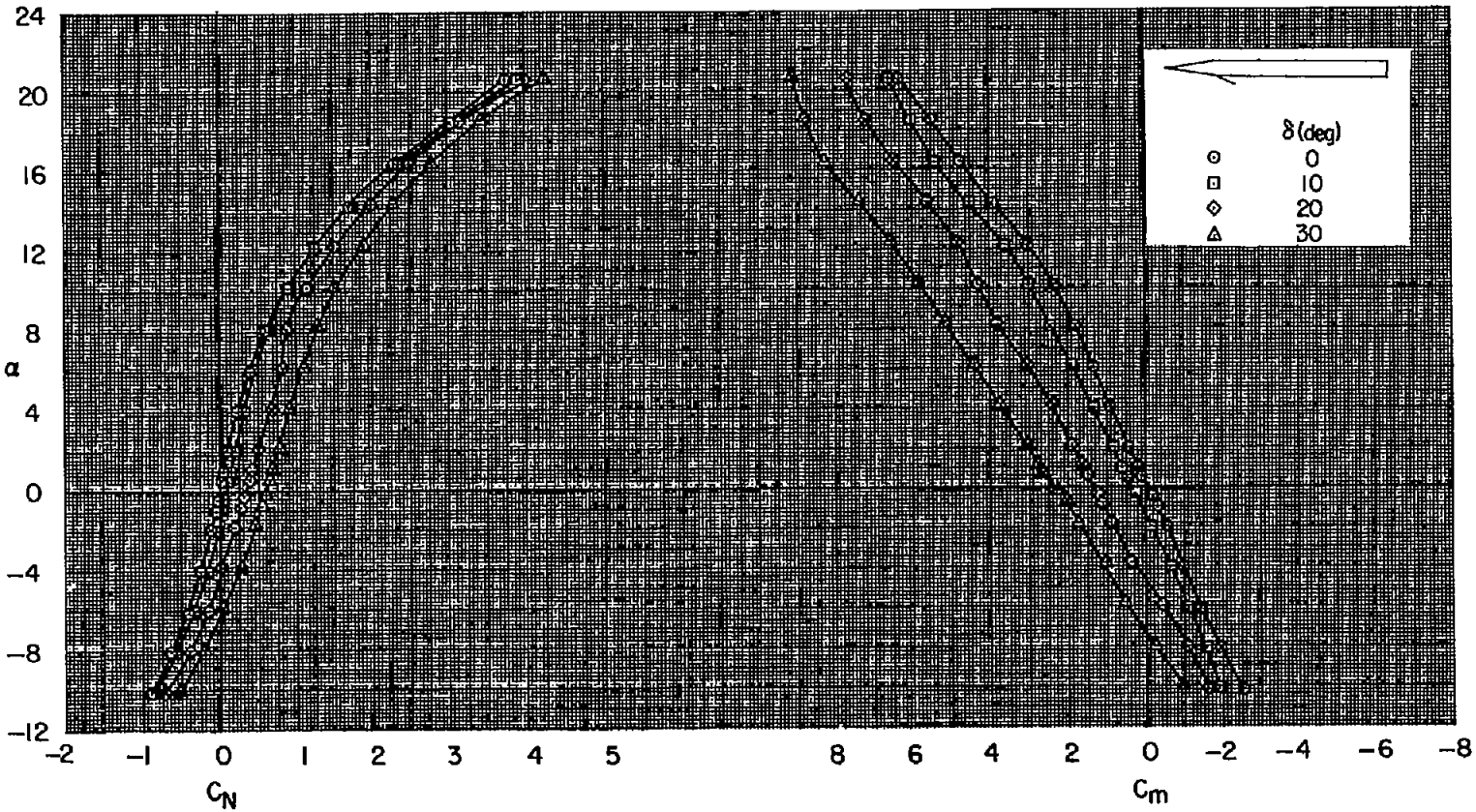

(b) M = 1.9

Figure 6.- Concluded.

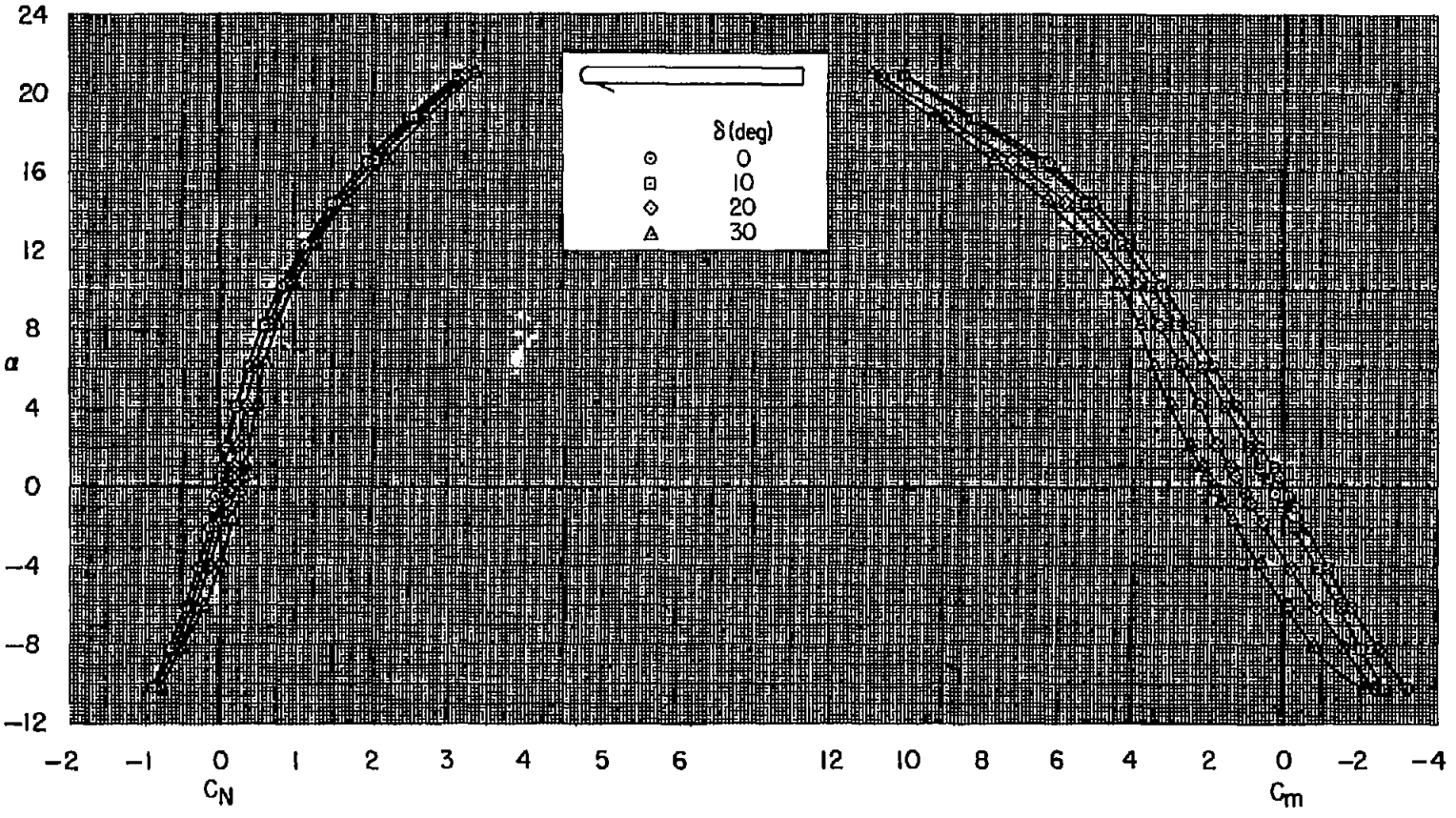

(a) M = 1.2

Figure 7.- Normal-force and pitching-moment characteristics of model E.

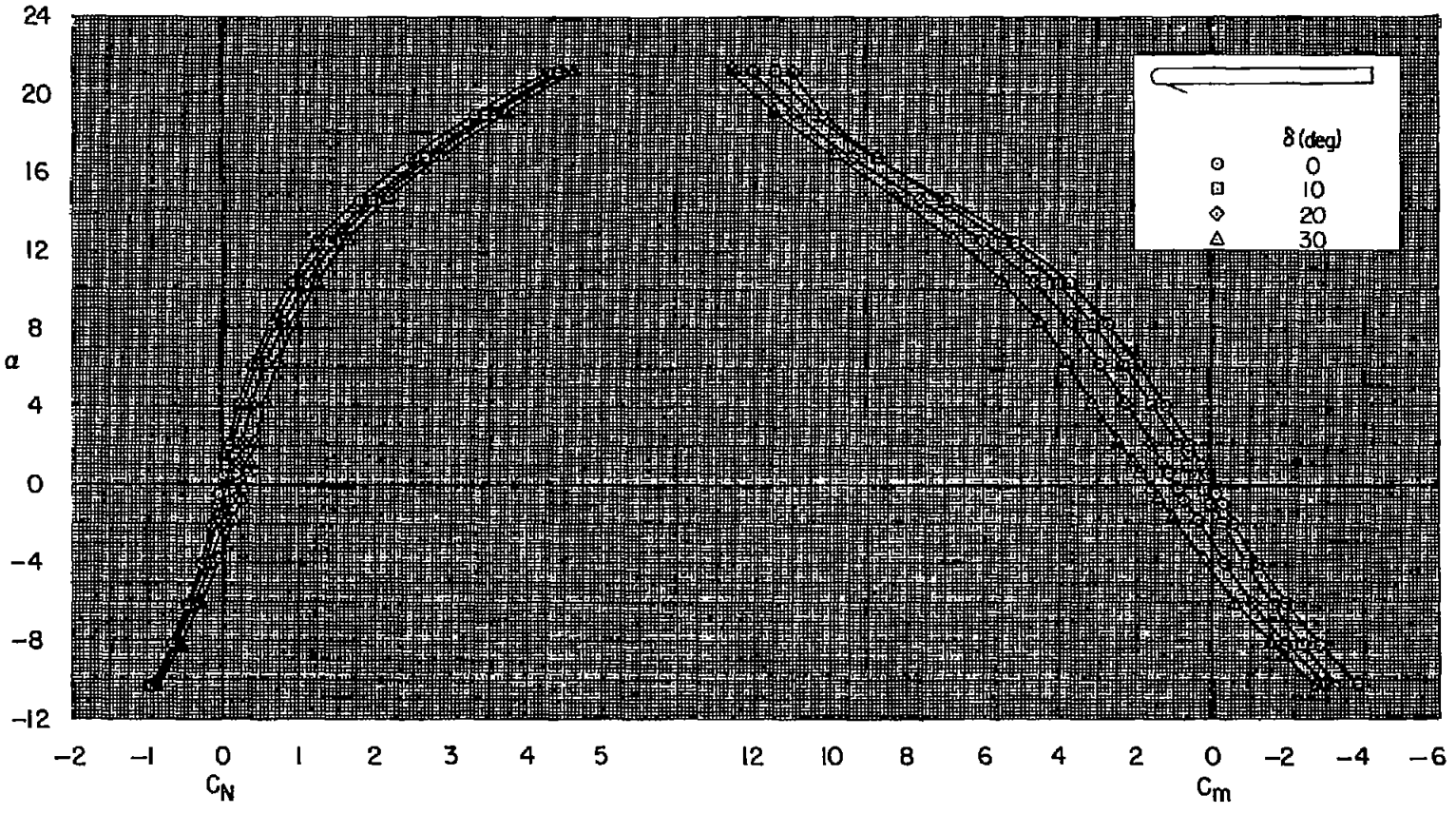

(b) M = 1.9

Figure 7.- Concluded.

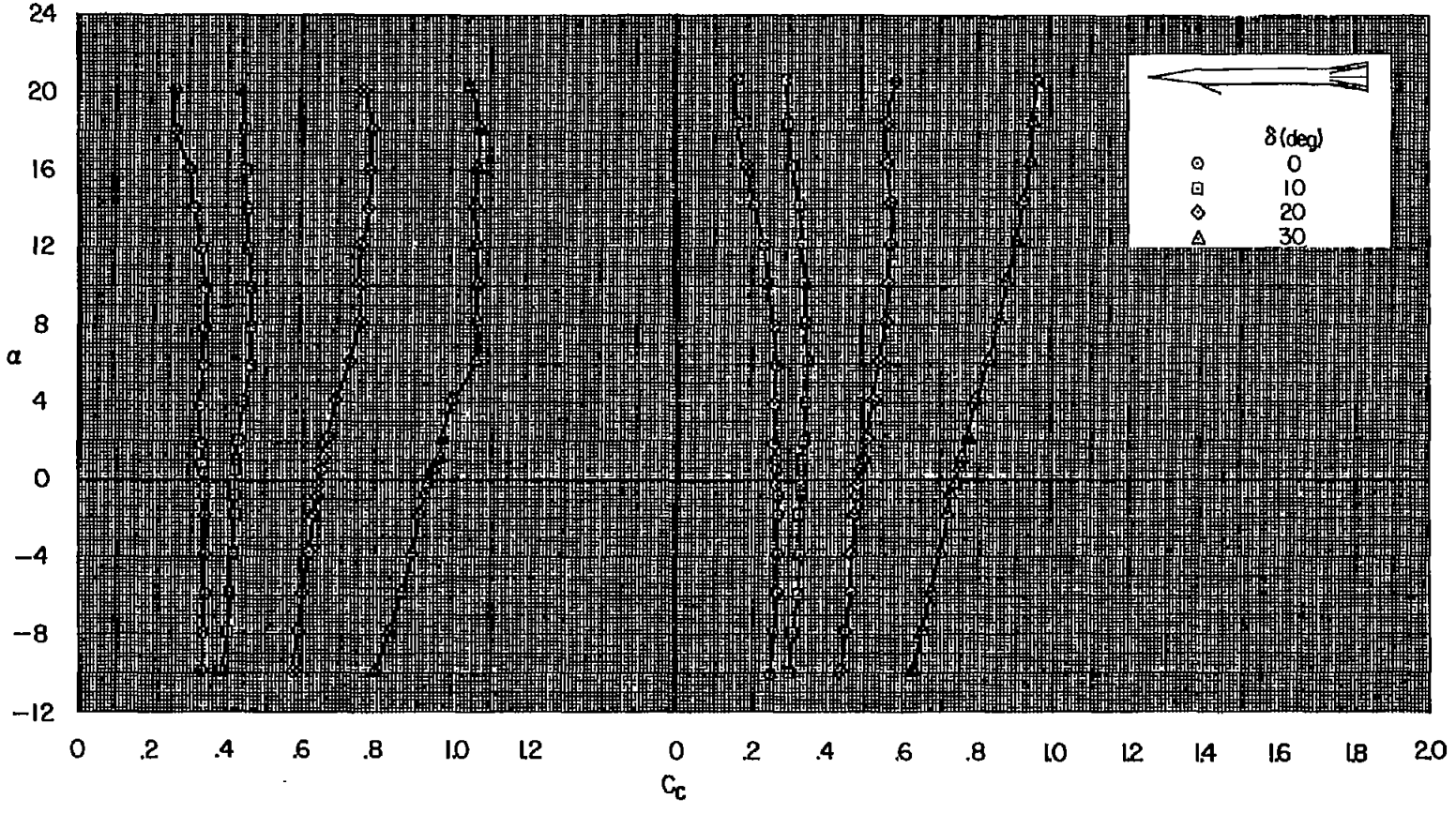

(a) Model A.

Figure 8.- Variation of axial-force coefficient with angle of attack for all configurations.

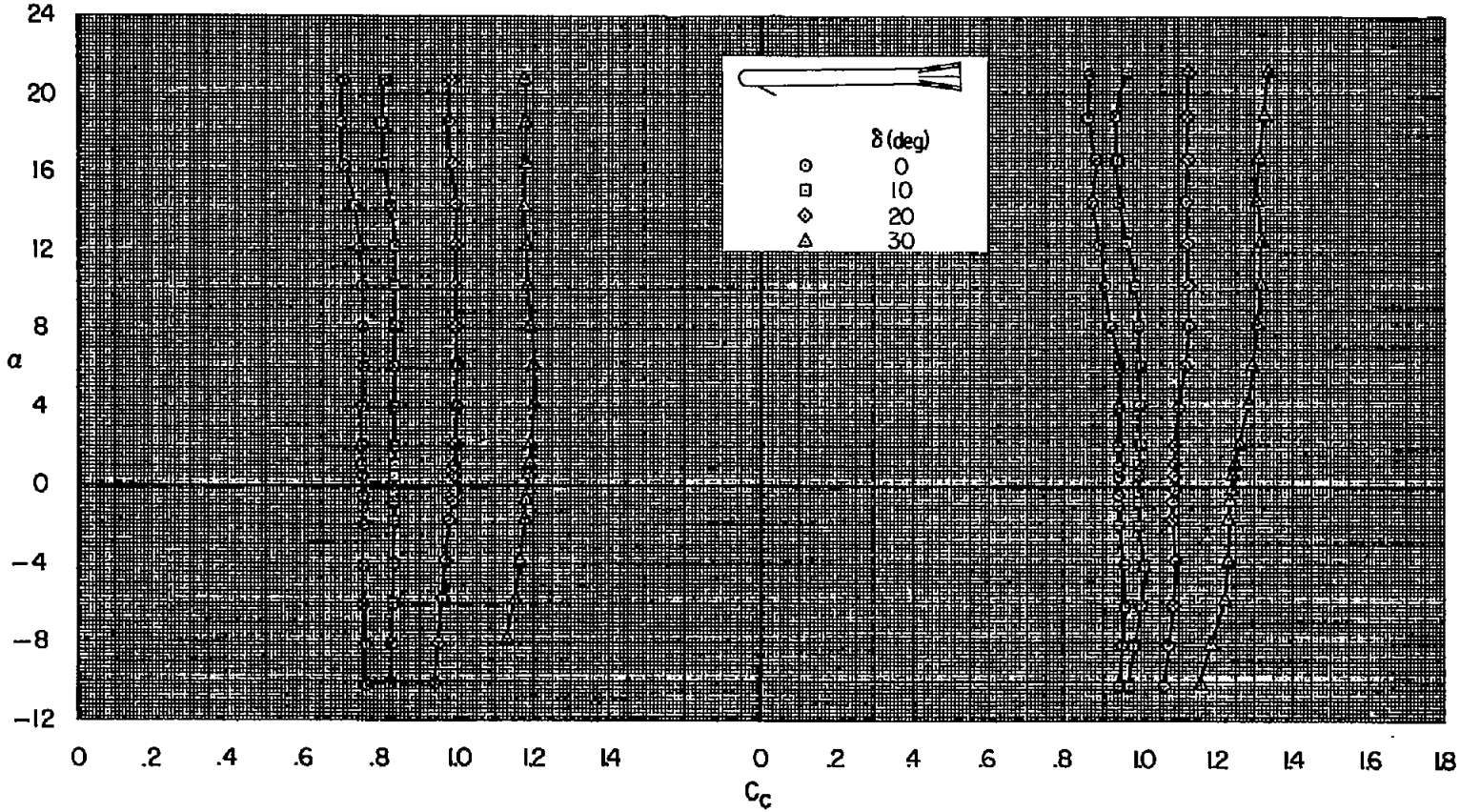

(b) Model C.

Figure 8.- Continued.

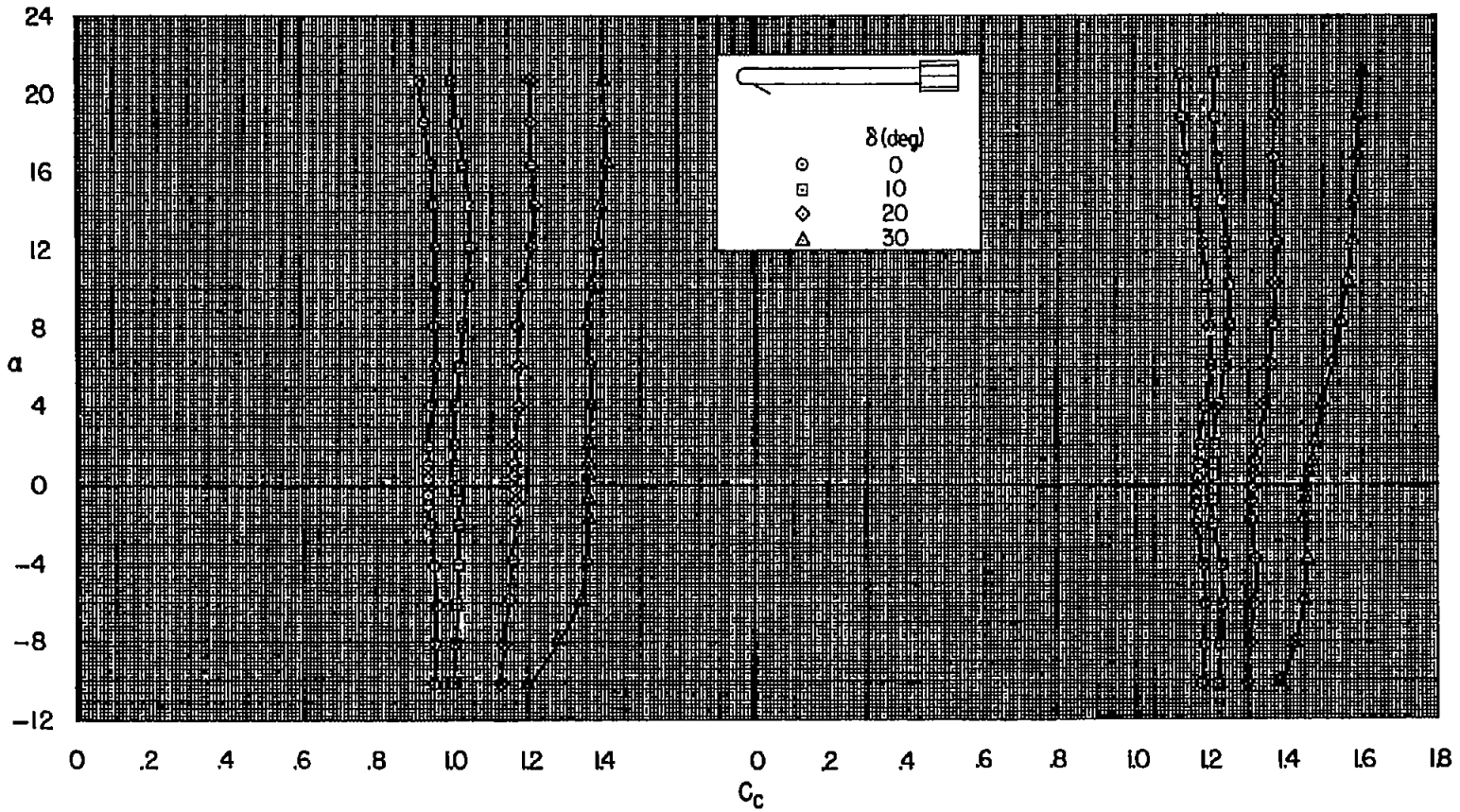

(c) Model D.

Figure 8.- Continued.

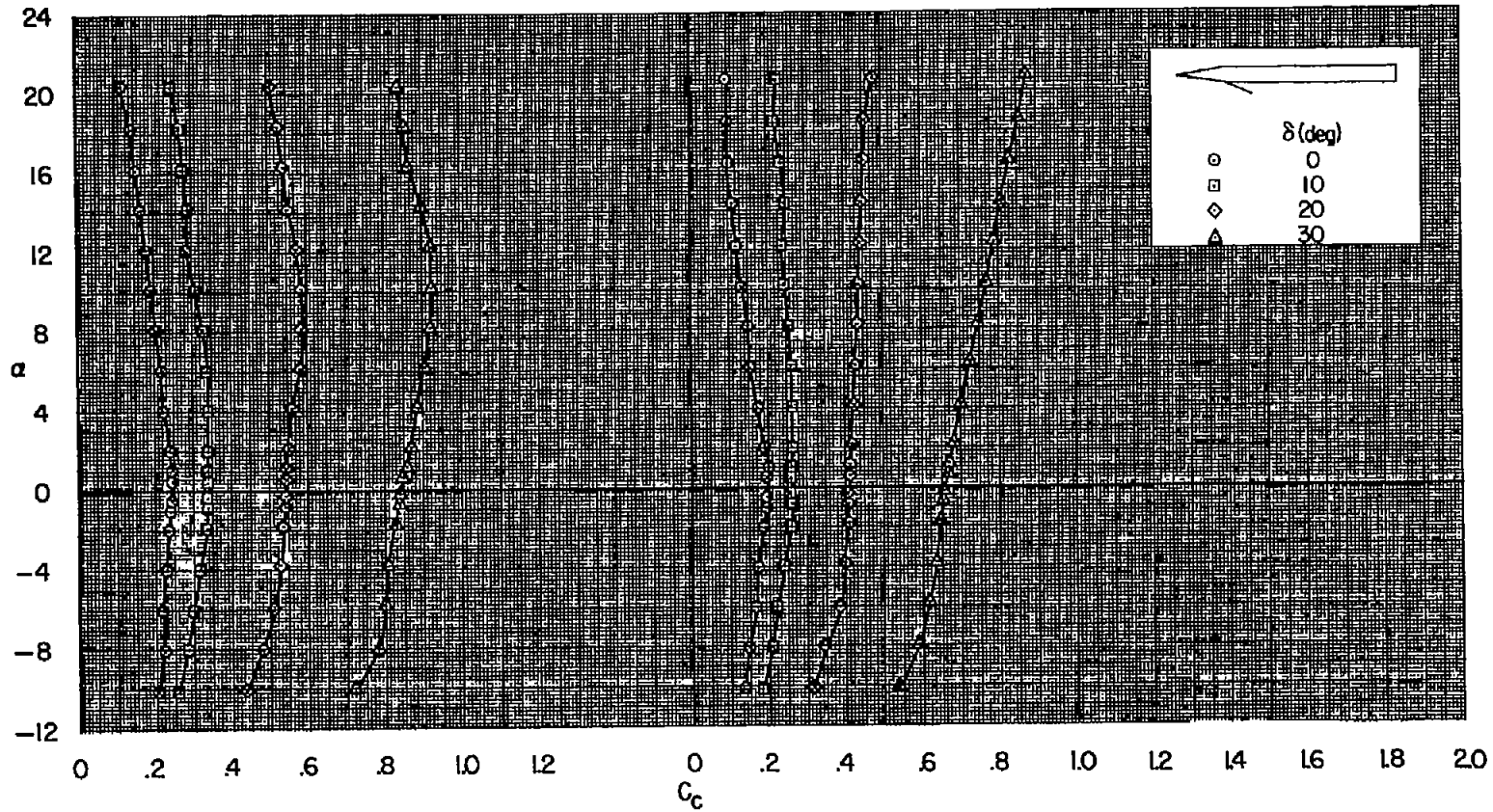

(d) Model B.

Figure 8.- Continued.

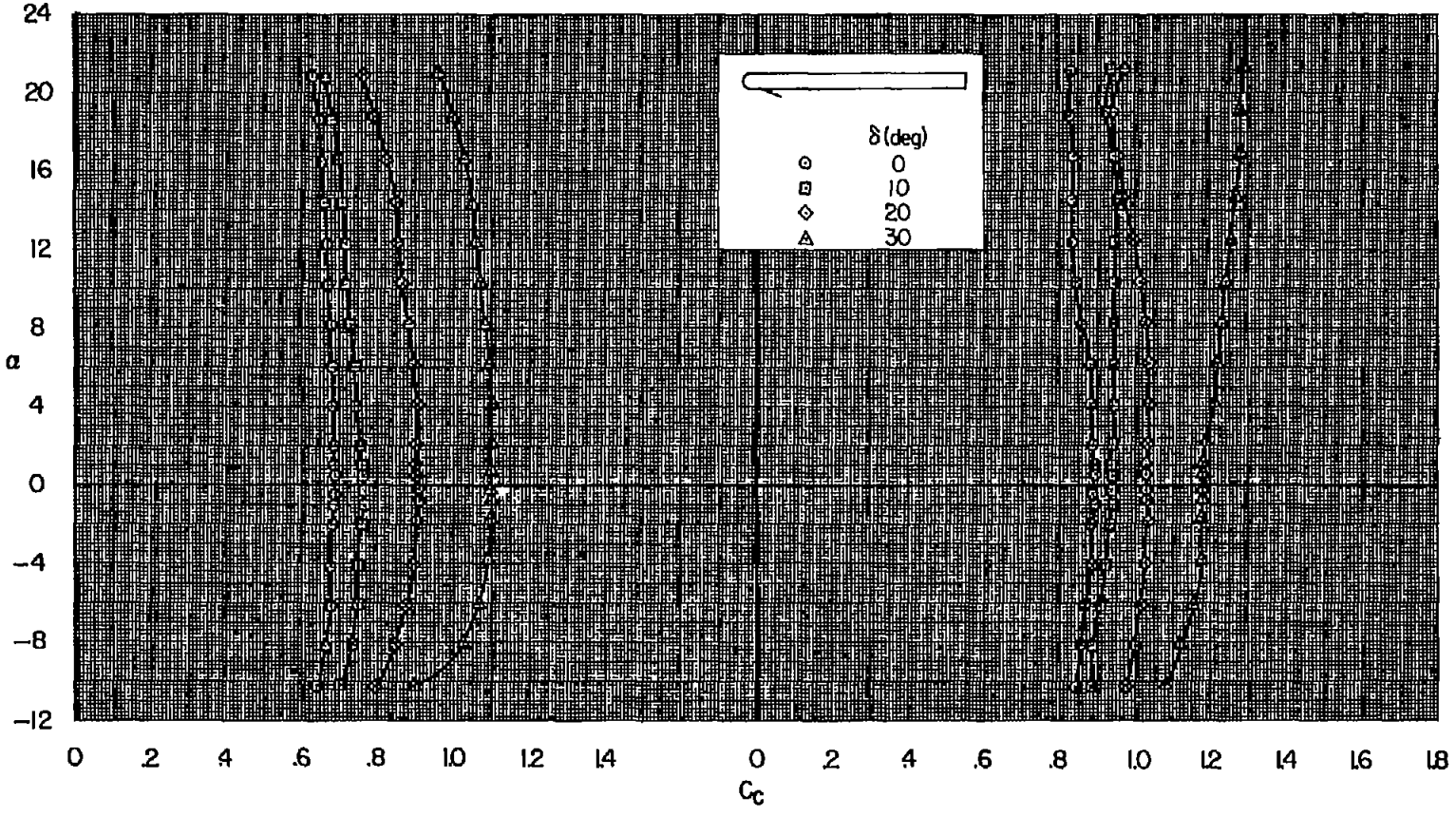

(e) Model E.

Figure 8.- Concluded.

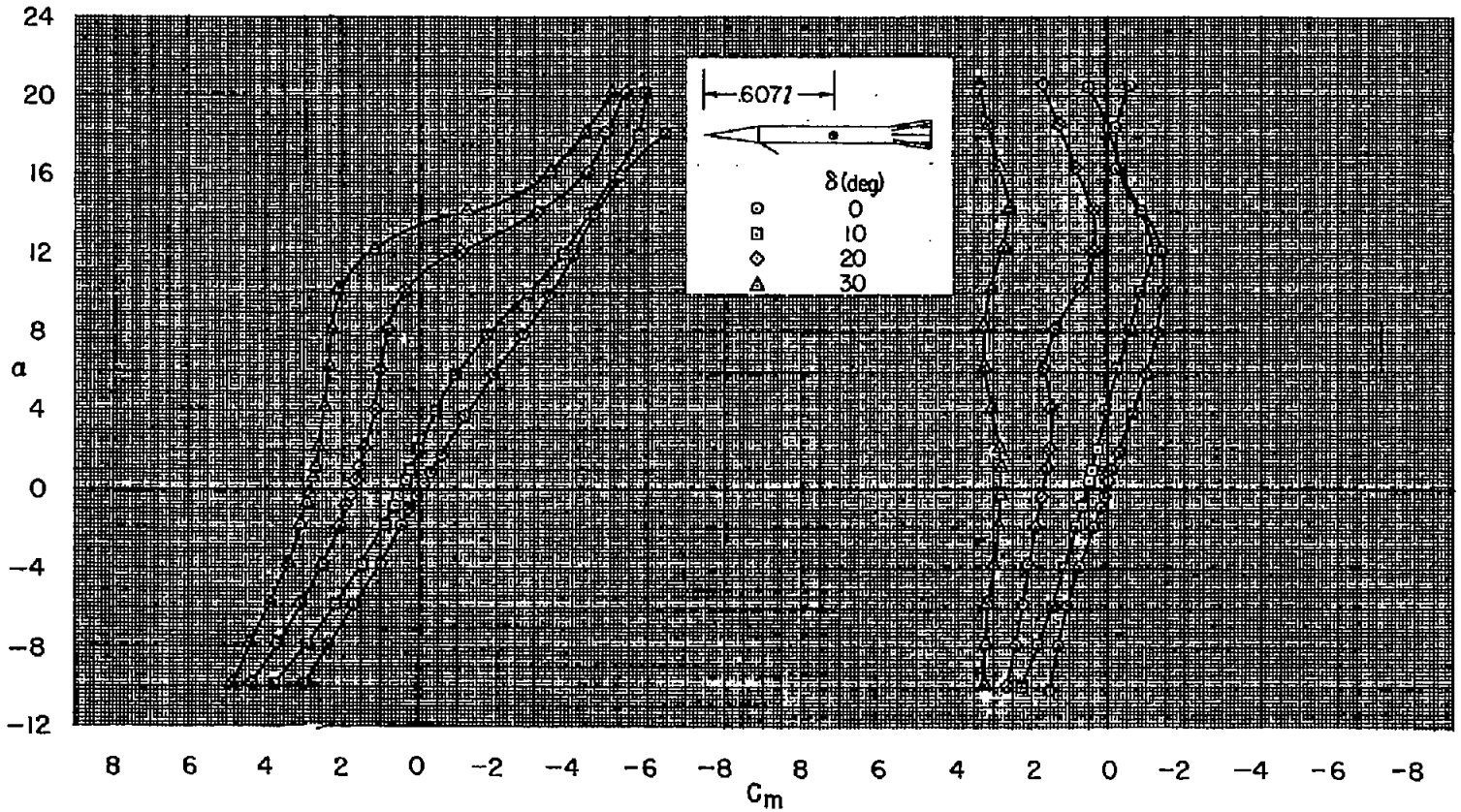

(a) Model A.

Figure 9.- Pitching-moment characteristics of the tail-on configurations for adjusted center-of-gravity positions.

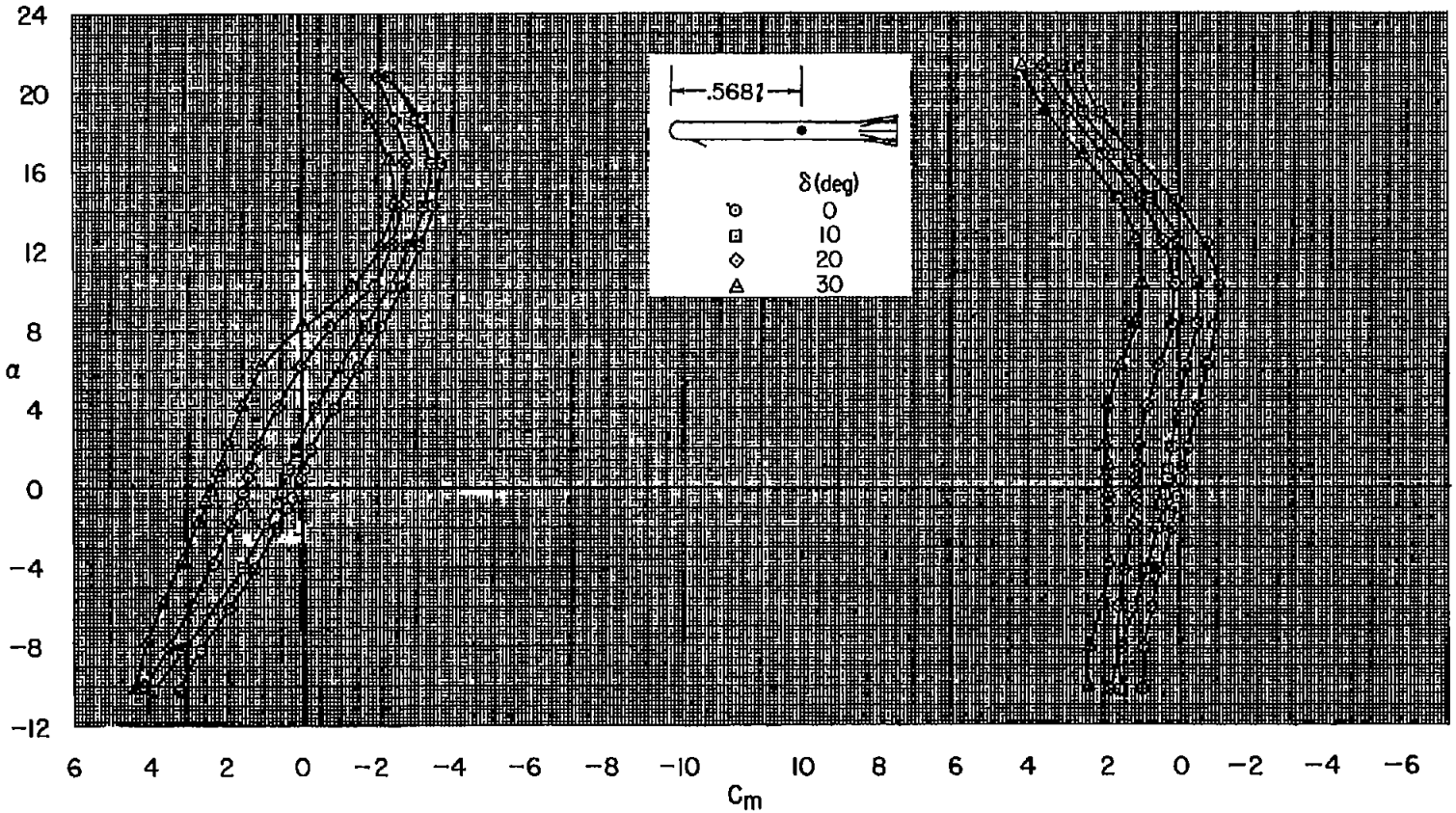

(b) Model C.

Figure 9.- Continued.

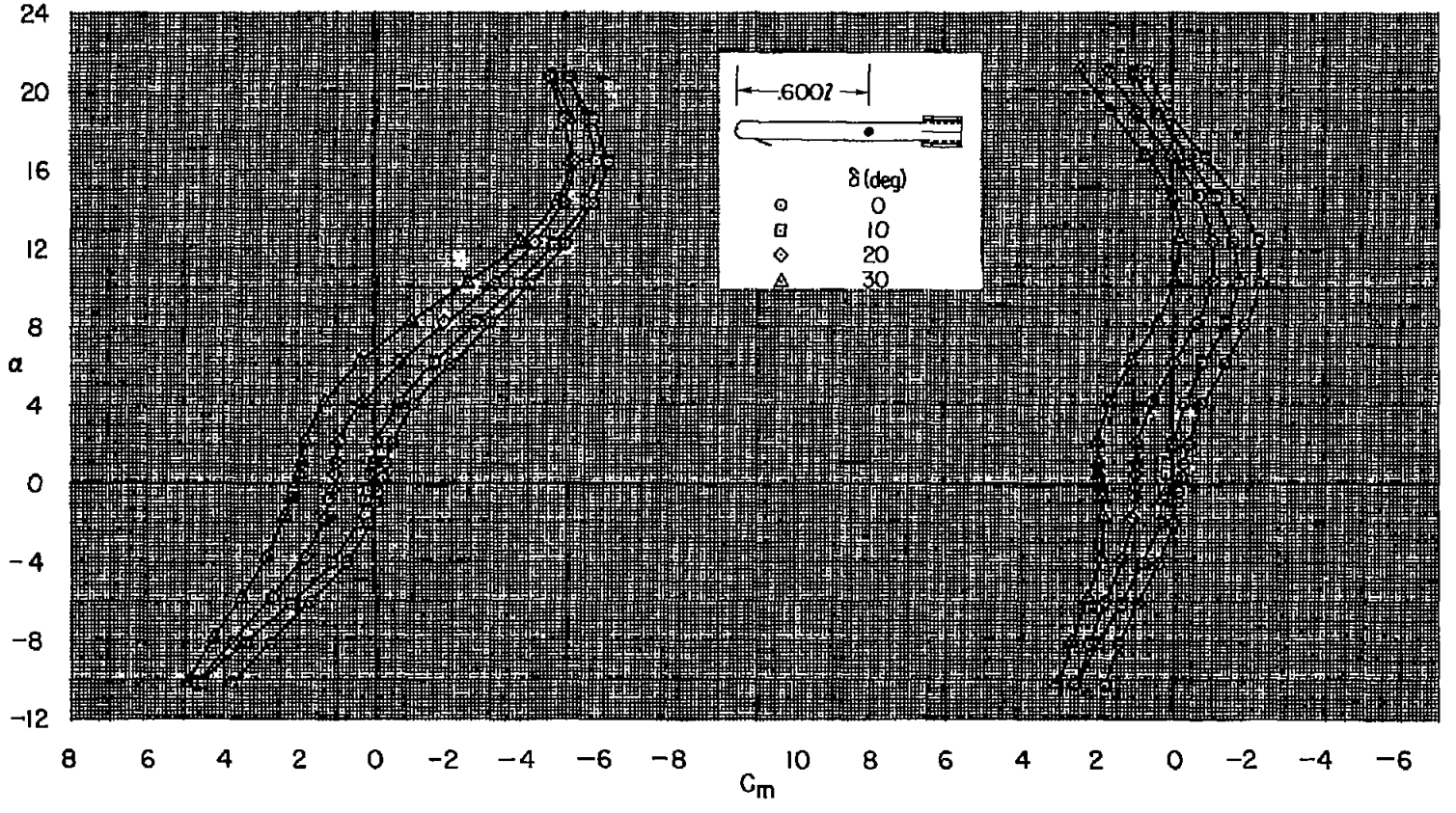

(c) Model D.

Figure 9.- Concluded.

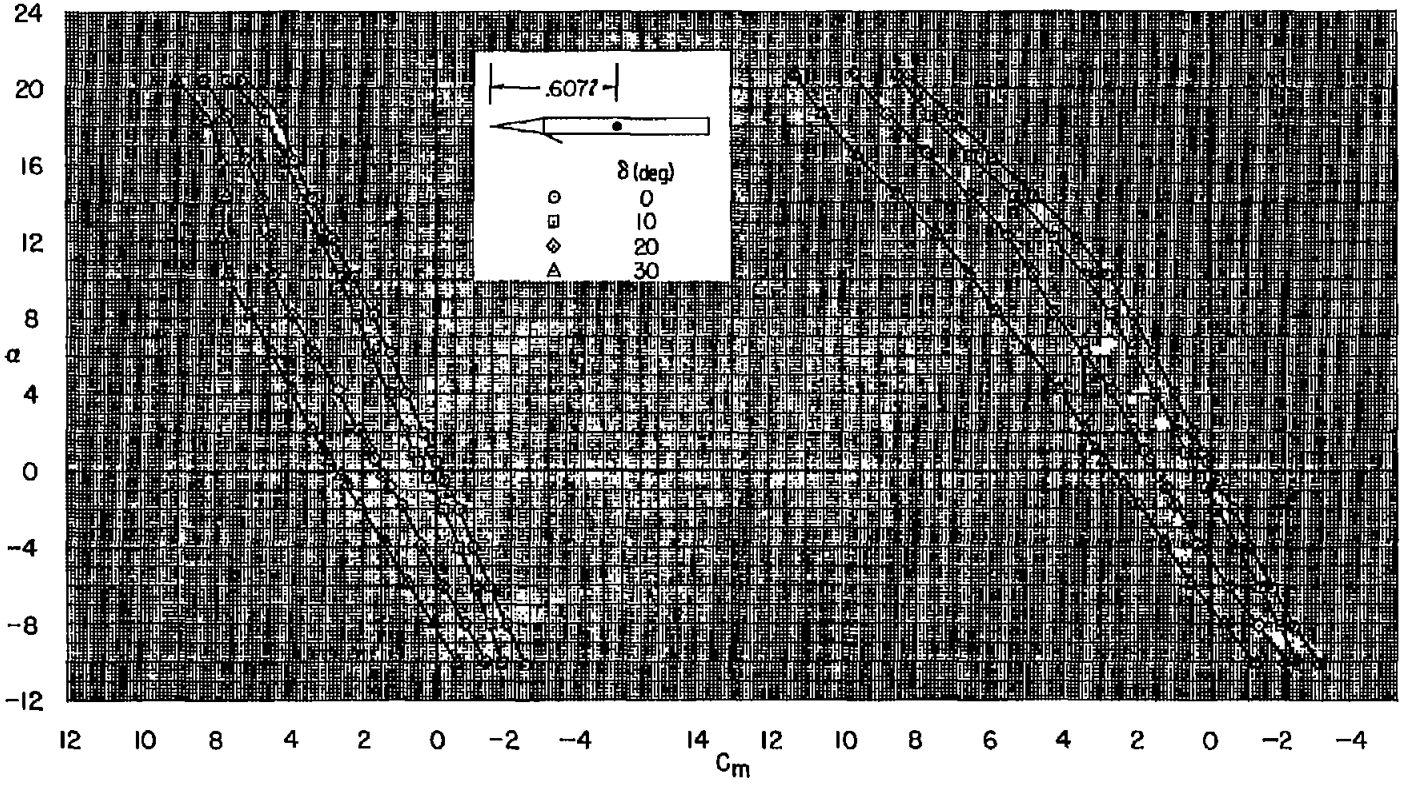

(a) Model B.

Figure 10.- Pitching-moment characteristics of the tail-off configurations for adjusted center-of-gravity positions.

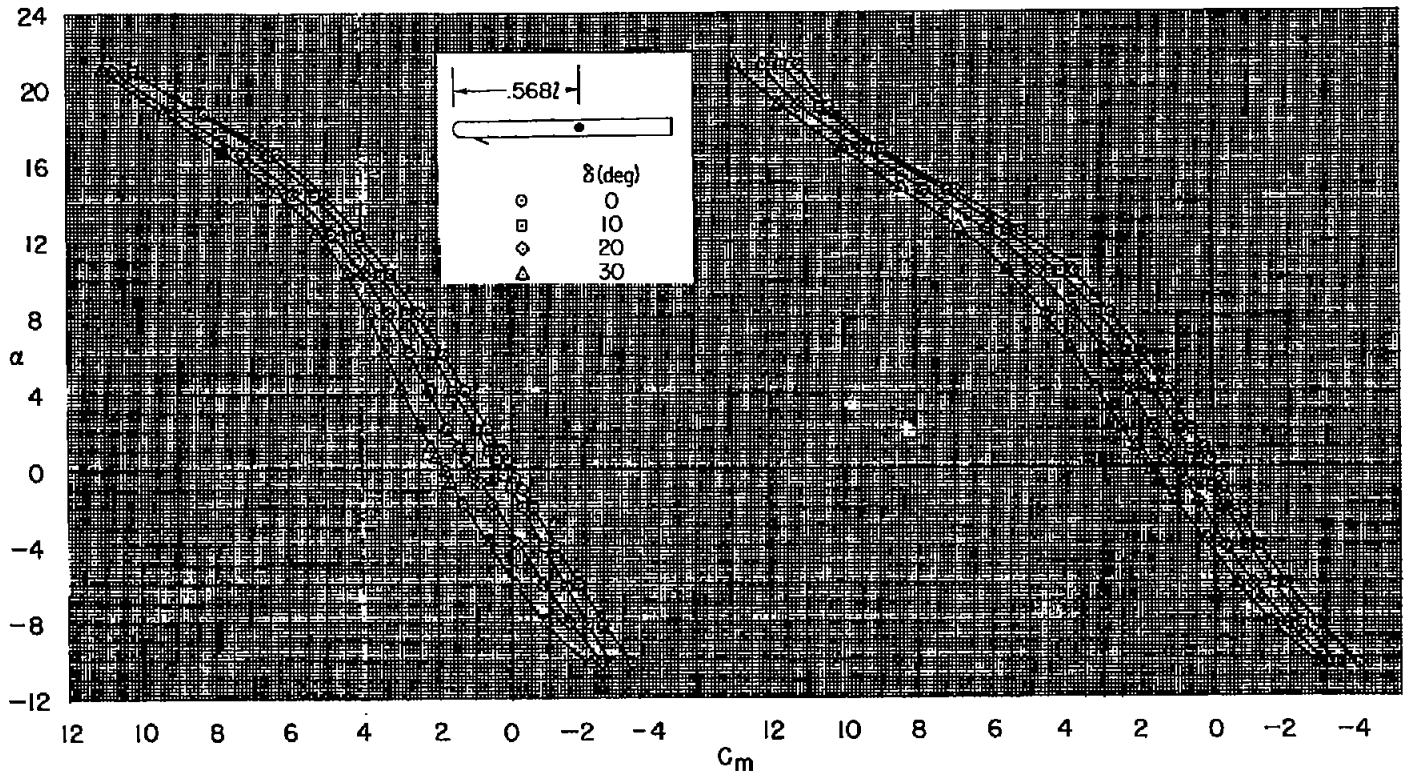

(b) Model E (model C with tail removed).

Figure 10.- Continued.

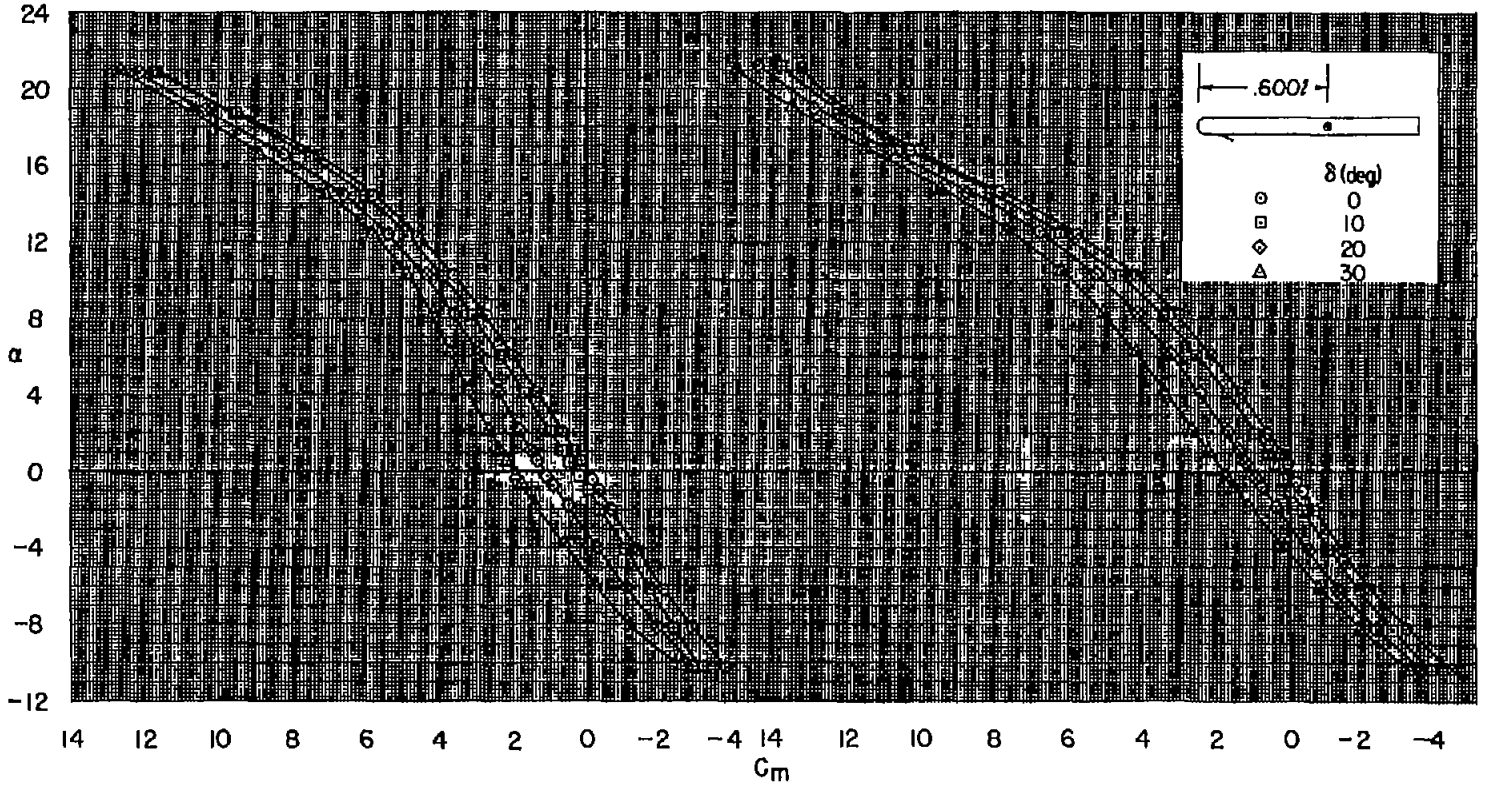

(c) Model E (model D with tail removed).

Figure 10.- Concluded.

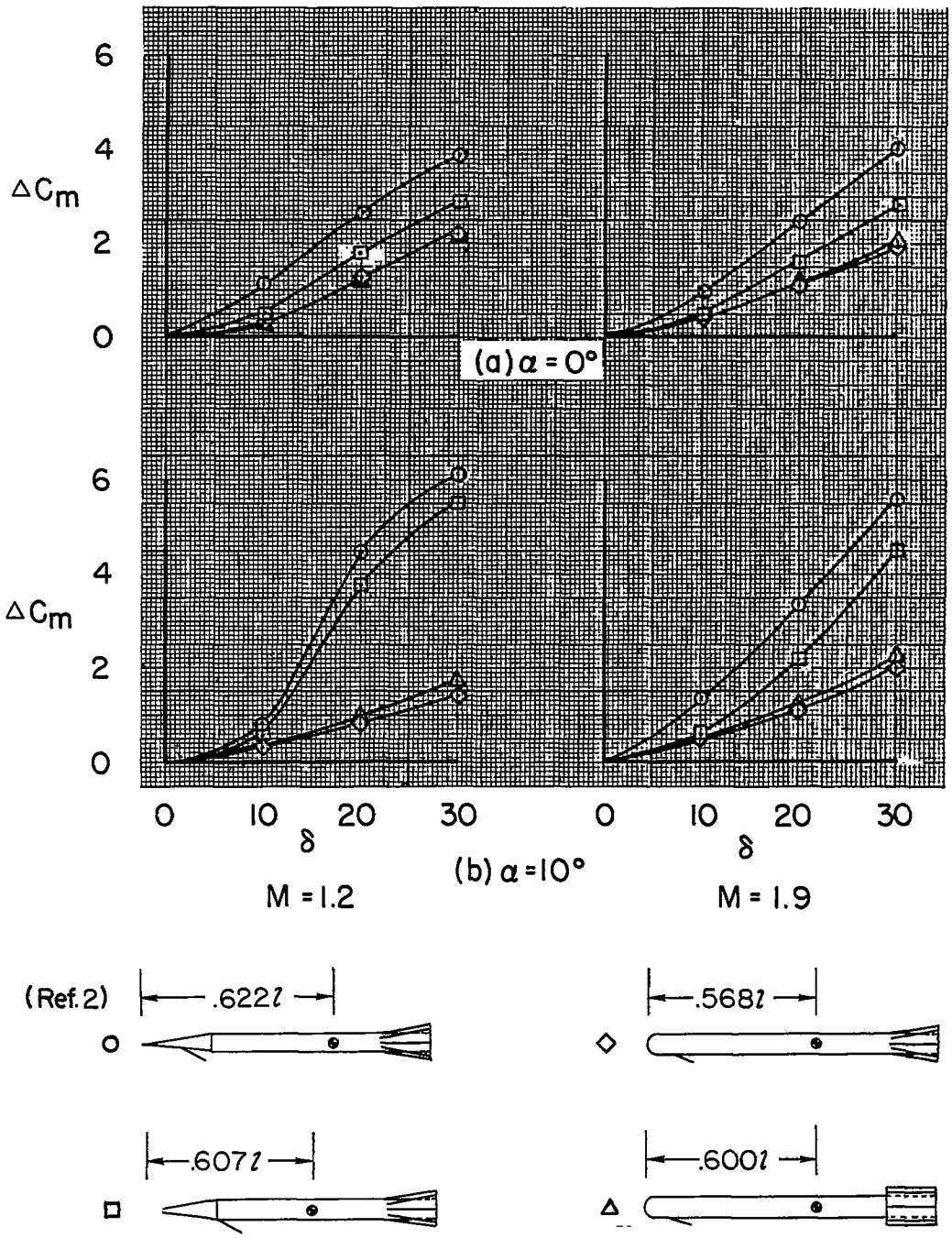

Figure 11.- Control effectiveness for the tail-on configurations.

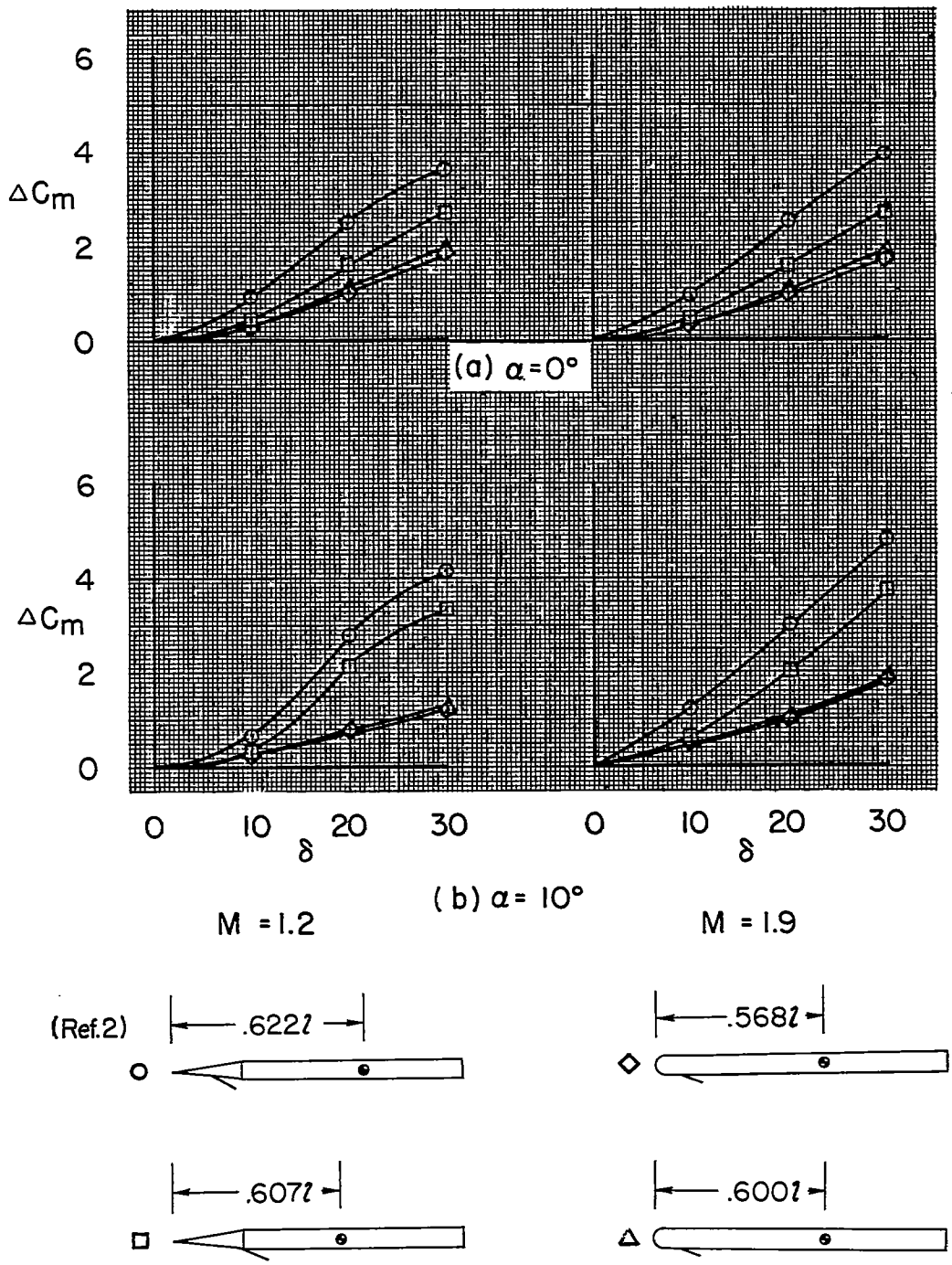

Figure 12.- Control effectiveness for the tail-off configurations.